Proceedings of the ASME 2019 Summer Heat Transfer Conference
HT2019
July 15-18, 2019, Bellevue, WA, USA

HT2019-3597

# MODEL AND SENSITIVITY ANALYSIS OF THE RECIPROCATING BIOMASS CONVERSION REACTOR (RBCR)

**Roshan Adhikari***
Graduate Student
Department of Mechanical Engineering
Stevens Institute of Technology
Hoboken, New Jersey 07030
Email: radhika2@stevens.edu

**Nick J. Parziale**
Assistant Professor, Member of ASME
Department of Mechanical Engineering
Stevens Institute of Technology
Hoboken, New Jersey 07030
Email: nparzial@stevens.edu

## ABSTRACT

The capabilities of a pilot-scale reciprocating biomass conversion reactor (RBCR) and its sensitivity to changes in various input parameters are examined. The RBCR is a 4-stroke diesel engine repurposed as a novel reactor to produce bio-oil by fast-pyrolysis of biomass. An external source powers the RBCR through the intake, compression/heating, expansion and exhaust strokes. Biomass is carried to the RBCR by an inert gas and is converted during compression as part of the compression work provides the heat of pyrolysis. A control-volume energy balance is coupled with a biomass decomposition mechanism from literature to predict the evolution of bio-products during compression and expansion strokes. The RBCR calculations are compared to experimental results from the state of the art considered to be a lab-scale fluidized-bed reactor (FBR). Calculations predict that the RBCR will increase the biomass throughput, and decrease the energy requirement for biomass conversion with a 6.8 times return on energy investment. The sensitivity analysis indicates the need for finely pulverized biomass for significant conversion, and highlights the versatility of the RBCR since operation parameters can be adjusted to achieve near complete conversion to bio-gas or to yield bio-oil up to 70% of biomass weight.

## 1 INTRODUCTION

Fast pyrolysis is a process where biomass is decomposed in an environment without an oxidizing agent at temperatures of approximately 500°C for short times. Thermochemical biomass conversion by fast pyrolysis to bio-oil, bio-char, and bio-gas is a part of an attractive path to an alternative energy source because of the upgrade in heating value and density [1] so that it may be easily transported as part of a new distribution network [2, 3]. Effective methods of biomass conversion to bio-oil are of interest because bio-oil represents a deployable energy carrier with favorable source characteristics (e.g., in-situ production and carbon-neutral) [4–9]. Biomass is pulverized, pyrolyzed, and the bio-products are recovered (Fig. 1). Bio-oil can be used directly in boilers (i.e., for heating or electricity), or upgraded for use as a fuel [2].

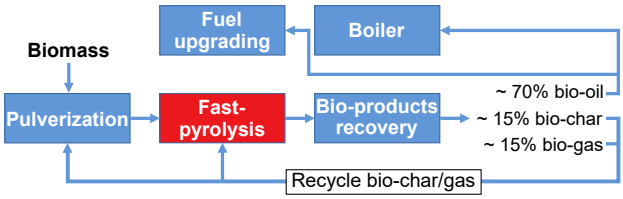


**FIGURE 1**. Flow chart for thermochemical conversion of biomass by fast pyrolysis. The approximate fractions of bio-products are taken from the literature [10].

There are a number of reactor types for fast pyrolysis: entrained flow reactor, wire mesh reactor, vacuum furnace reactor, vortex reactor, rotating reactor, microwave reactor, fluidized-bed reactor, and the circulating fluidized-bed reactor [10–20].

The fluidized-bed reactor (FBR) is representative of the current state of the art. The FBR requires a condenser to cool the bio-products to quench the secondary pyrolysis reactions [16]. The condenser is an active cooling component that leads to heat loss and system inefficiency. The primary pyrolysis reactions create the pyrolysis vapor which condenses to bio-oil; the secondary pyrolysis reactions adversely affect the bio-oil quality and should be avoided [1, 10, 12, 16, 21].

In this work, we describe a novel reactor for the conversion of biomass that can reduce energy requirements and rapidly quench unwanted secondary pyrolysis reactions. It is termed the

*Address all correspondence to this author.

'reciprocating biomass conversion reactor' (RBCR). At its essence, the conversion scheme is a high compression-ratio motor being cycled by an external power source to efficiently provide process heat to biomass. A model is presented for the decomposition of multi-component biomass in an RBCR. Specifically, bagasse decomposition for the compression and expansion strokes of the RBCR is described. Additionally, a sensitivity study is presented by fixing all but one parameter among engine speed, biomass particle diameter, biomass feed-rate, and biomass composition.

## 2 RECIPROCATING BIOMASS CONVERSION REACTOR (RBCR)

The reciprocating biomass conversion reactor (RBCR) cycle utilizes rapid heating/conversion and cooling of a small volume-fraction of pulverized biomass suspended in a non-oxidizing gas within a cylinder [22, 23]. The process flowchart is presented in Fig. 2. In a typical Diesel engine, the 4-stroke cycle is: intake, compression, power, and exhaust; in the proposed conversion scheme, this is replaced with: intake, compression/heating, expansion, and exhaust. The idealized cycle for the proposed biomass conversion scheme proceeds as follows:

1. *Intake:* A two-phase mixture of an inert fluidizing gas ($Ar$, $N_2$, or a $CO/CO_2$ mixture) and a small volume-fraction of pulverized biomass are input into the cylinder of a high compression-ratio engine.
2. *Compression/heating:* An external power source (e.g., an electric motor) turns the crankshaft driving the piston to compress and heat the biomass/ fluidizing-gas mixture within the cylinder. Process heat is transferred from the fluidizing gas to the biomass, primarily by convection; this process heat is sufficient to thermochemically convert the biomass to bio-products by fast pyrolysis.
3. *Expansion/cooling:* The expansion stroke rapidly decreases the temperature and pressure of the fluidizing-gas/ bio-products mixture within the cylinder, quenching the undesirable secondary pyrolysis reactions. A significant fraction of the energy required to compress the system is recovered as the pressure is reduced through expansion. The recovered energy may be used on the compression stroke of another cylinder on the same crankshaft.
4. *Exhaust:* The exhaust stroke forces the fluidizing-gas/ bio-products mixture from the cylinder.

This cycle has the potential to reduce operating costs of thermochemical conversion by reducing the required input energy to the system and improving the quality of the bio-products by quenching undesirable secondary pyrolysis reactions. The instant following desired biomass conversion, the bio-products and fluidizing gas reside within the cylinder at an elevated temperature and pressure. This is surplus process heat, and in contrast to the state of the art, the surplus process heat is transferred and reused mechanically through the crankshaft to another piston/cylinder during the expansion stroke. In the following sections, we present a model to predict the useful biomass conversion parameter space of the RBCR.

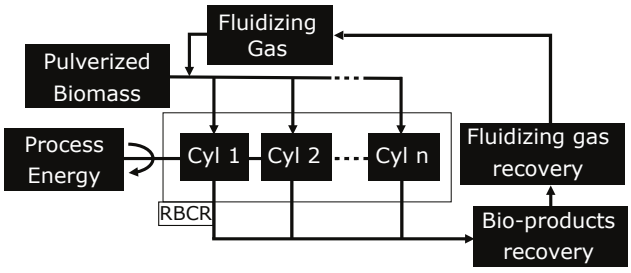


**FIGURE 2**. Reciprocating Biomass Conversion Reactor (RBCR) process flowchart.

## 3 CLOSED CONTROL-VOLUME ENERGY BALANCE

Here, we analyze a closed control volume, presented as Fig. 3, which surrounds one cylinder of the RBCR shown in Fig. 2. There is a well-mixed and evenly distributed fluidizing gas and biomass/bio-products mixture in this control volume; the fluidizing gas and biomass are separated in Fig. 3 only to clearly show the direction of energy transfer. In Fig. 3, $Q$ is the energy that is transferred into a control volume by heat transfer, $W$ is is the energy that is transferred out of a control volume by work, and $\Delta H_P$ is the change in enthalpy required to pyrolyze the biomass. The subscripts $b$, $g$, and $w$ represent the biomass, fluidizing gas, and wall, respectively. Two subscripts in succession indicate "from $a$ to $b$," e.g., $Q_{gb}$ is the energy transferred from the fluidizing gas to the biomass by heat transfer. Additionally, we assume that the pressure of the fluidizing gas and biomass are equal, $P_g = P_b = P$.

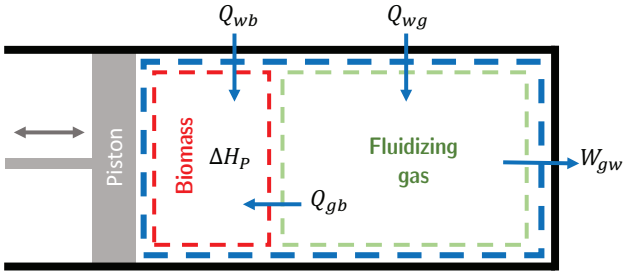


**FIGURE 3**. Control volume for analysis of the compression and expansion strokes of the RBCR. The red marks the control volume for the biomass, the green marks the control volume for the fluidizing gas, and the blue marks the control volume enclosing the cylinder for one cycle. We assume a well-mixed and evenly distributed fluidizing gas and biomass/bio-products mixture in this control volume; they are separated only to clearly show the direction of energy transfer.

The change in internal energy for the fluidizing gas is $\Delta U_g = c_{vg} n_g \Delta T_g$ and the work term is $W_{gw} = P\Delta V_g$. Here, $c_{vg}$, $n_g$, $\Delta T_g$, and $V_g$ are the constant-volume molar specific heat, number of moles, change in temperature, and volume of the fluidizing gas, respectively. The first law for the control volume of the fluidizing-gas is written as

$$\begin{aligned} \Delta U_g &= Q_g - W_g = -Q_{gb} + Q_{wg} - W_{gw} \\ \Delta U_g &= c_{vg} n_g \Delta T_g = -Q_{gb} + Q_{wg} - P\Delta V_g. \end{aligned} \tag{1}$$

The change in enthalpy of the biomass, $\Delta H_b$, includes the change in sensible enthalpy, $\Delta H_S$, and enthalpy of pyrolysis reactions, $\Delta H_P$, as $\Delta H_b = \Delta H_S + \Delta H_P = \Delta U_b + \Delta(PV_b)$. We assume that there is no volumetric change of the biomass. The change in enthalpy due to pyrolysis is $\Delta H_P = m_P \Delta h_P$, and the change in sensible enthalpy is $\Delta H_S = m_b c_b \Delta T_b$. Here $m_p$, $\Delta h_P$, $m_b$, $c_b$, and $\Delta T_b$ are the pyrolyzed mass, mass-specific enthalpy of pyrolysis, biomass mass, biomass mass-specific heat, and change in biomass temperature, respectively. The first law for the control volume for the biomass is written as

$$\begin{aligned} \Delta U_b &= Q_b - W_b = Q_{gb} + Q_{wb} - W_b \\ \Delta U_b &= m_b c_b \Delta T_b + m_P \Delta h_P - V_b \Delta P = Q_{gb} + Q_{wb} \end{aligned} \tag{2}$$

## 4 IDEAL MODEL AS EXPLANATION OF RBCR CYCLE

We can create a simple model of biomass decomposition in an RBCR to illustrate its utility and working principles. Heat transfer to the RBCR walls is not considered, $Q_{wb} = Q_{wg} = 0$, and all the biomass is pyrolyzed: $m_P = m_b$. Additionally, the change in pressure term is considered to be small for the biomass solid, $V_b \Delta P \ll m_b c_b \Delta T_b$, and $V_b \Delta P \ll m_P \Delta h_P$. Eqs. 1 and 2 are rewritten as

$$\Delta T_g = -\frac{Q_{gb} + P\Delta V_g}{c_{vg} n_g}, \tag{3}$$

and,

$$Q_{gb} = m_b c_b \Delta T_b + m_b \Delta h_P. \tag{4}$$

The fluidizing gas of an RBCR is presented in pressure-volume and temperature-state space in Fig. 4. In that figure, the states 1-4 are label and undergo:

1. **1-2** Isentropic compression of the fluidizing gas, requiring $W_{in}$. The compression is fast relative to any possible heat transfer process, so $Q_{gb} = \Delta T_b = 0$.
2. **2-3** Isobaric heat transfer from the fluidizing gas to the biomass for conversion, $Q_{gb}$. The biomass undergoes "complete" conversion at a specified temperature typical of fast pyrolysis.
3. **3-4** Isentropic expansion of the fluidizing gas, extracting, $W_{out}$. The expansion is fast relative to any possible heat transfer process, so $Q_{gb} = \Delta T_b = 0$.
4. **4-1** Isochoric heat transfer from the biomass to the fluidizing gas, $Q_{gb}$. This quenches the undesirable secondary pyrolysis reactions.

## 5 TRANSIENT RBCR CONTROL VOLUME

A more detailed treatment will be presented in this section to predict the transient response of the RBCR. Differential equations are formulated from the application of the first law to the fluidizing gas and the biomass/bio-products in the reactor

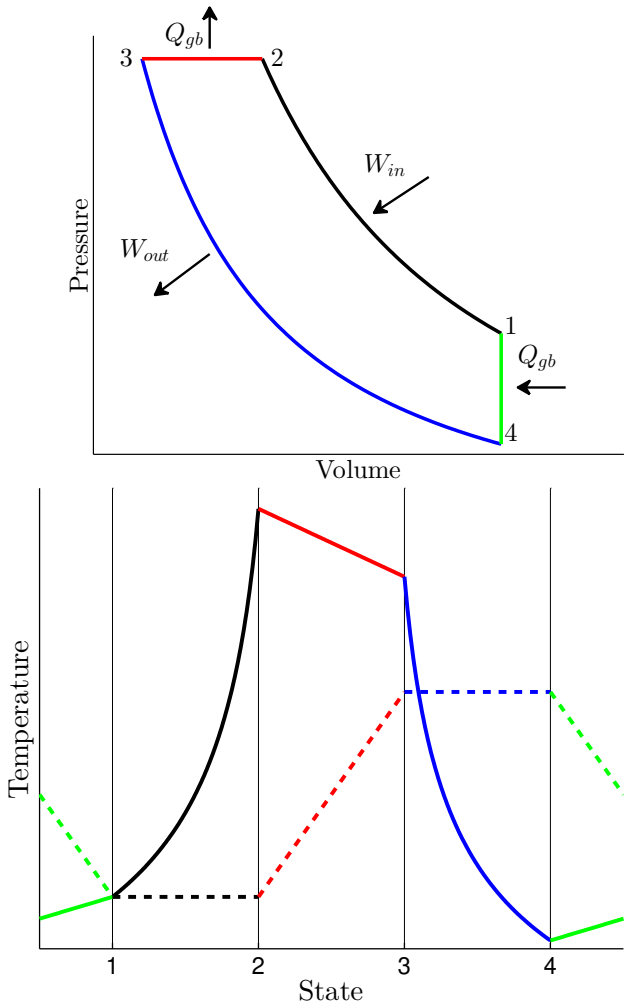


**FIGURE 4**. *Top:* RBCR cycle of fluidizing gas in pressure-volume space. Cycle proceeds counter clockwise. 1-2: $W_{in}$ is the work required for isentropic compression of the fluidizing gas. 2-3: $Q_{gb}$ is the isobaric heat transfer from the fluidizing gas to the biomass. 3-4: $W_{out}$ is the work extracted by isentropic expansion of the fluidizing gas. 4-1: $Q_{gb}$ is isochoric heat transfer from the biomass to the fluidizing gas. *Bottom:* RBCR cycle in temperature-state space. Solid lines represent the fluidizing-gas temperature. Dashed lines represent the biomass temperature.

(Eqs. 1 and 2). The time-rate form of Eq. 1 is

$$\frac{dT_g}{dt} = \left( -\dot{Q}_{gb} + \dot{Q}_{wg} - P\frac{dV_g}{dt} \right) / (c_{vg} n_g). \tag{5}$$

Inspection of Eq. 5 implies that the time-rate of change of temperature is increased by cylinder volume decrease and decreased by heat transfer to the surroundings. The $dV_g/dt$ term is prescribed by considering the kinematic motion of the piston [24].

The biomass is assumed to be a collection of independent spheres that act as a lumped mass, $m_b$, with specific heat $c_b$, and a constant volume. Individual fractions of $m_b$ are permitted to evolve as computed by the first-order kinetics mechanism reviewed in Xue et al. [25] (Fig. 5). Additionally, the rate of

energy loss due to pyrolysis, $\dot{Q}_{\Delta h}$, is included in the calculations. The collection of independent spheres act as a lumped mass; so, Eq. 2 can be rewritten to predict the biomass temperature ($T_b$) change as

$$\frac{dT_b}{dt} = \left( \dot{Q}_{gb} + \dot{Q}_{wb} - \Delta \dot{H}_P + V_b \frac{dP}{dt} \right) / (m_b c_b). \tag{6}$$

The $dP/dt$ term can be related to the time rate of change of the fluidizing-gas temperature and volume change through the differentiation of the logarithm of the ideal gas law as

$$\frac{dP}{dt} = P \left( \frac{1}{T_g} \frac{dT_g}{dt} - \frac{1}{V_g} \frac{dV_g}{dt} \right). \tag{7}$$

The emerging nature of the biomass pyrolysis modeling field (reviews in [18, 26–28]) presents a number of options to model the production rates of bio-products. We choose a model which "super poses" cellulose, hemicellulose, and lignin as

$$m_b = m_c + m_h + m_l, \tag{8}$$

where $m_c$, $m_h$, and $m_l$ are the individual masses of cellulose, hemicellulose, and lignin, respectively. The fractions of the biomass are defined as $\alpha = m_c/m_b$, $\beta = m_h/m_b$, and $\gamma = m_l/m_b$. The evolution of these fractions are modeled simultaneously and independently. Examples of different compositions are given in Table 1.

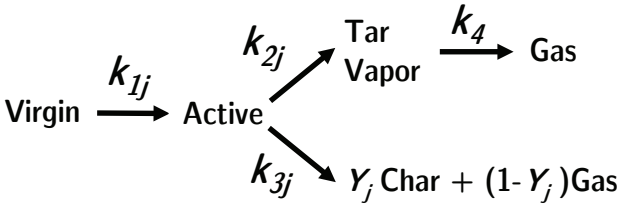


**FIGURE 5**. Mechanism for pyrolysis adapted from [25, 29–40]. $j$ may be cellulose $C$, hemicellulose $H$, or lignin, $L$.

The mechanism to predict the decomposition of biomass closely follows the development in references [25, 29–40]. In particular, the works by Xue et al. [25, 40] have resulted in a

**TABLE 1**. BIOMASS COMPOSITION FRACTION FROM [29]

| Feedstock | Cellulose | Hemicellulose | Lignin |
|---|---|---|---|
| Pure Cellulose | 1.00 | 0.00 | 0.00 |
| Bagasse | 0.36 | 0.47 | 0.17 |
| Oak | 0.35 | 0.40 | 0.25 |
| Olive Husk | 0.22 | 0.33 | 0.45 |

**TABLE 2**. INDICES OF EACH COMPONENT

| Component | Index |
|---|---|
| Virgin Cellulose | 1 |
| Virgin Hemicellulose | 2 |
| Virgin Lignin | 3 |
| Active Cellulose | 4 |
| Active Hemicellulose | 5 |
| Active Lignin | 6 |
| Tar Vapor | 7 |
| Gas | 8 |
| Char | 9 |

model which will be used for this work. The mechanism appears as Fig. 5, and pictorially depicts how the cellulose, hemicellulose, and lignin decompose. The indices for each component can be found in Table 2. The rates of change for the masses are written as

$$\dot{m}_1 = -k_{1C} m_1 \tag{9a}$$
$$\dot{m}_2 = -k_{1H} m_2 \tag{9b}$$
$$\dot{m}_3 = -k_{1L} m_3 \tag{9c}$$
$$\dot{m}_4 = k_{1C} m_1 - k_{2C} m_4 - k_{3C} m_4 \tag{9d}$$
$$\dot{m}_5 = k_{1H} m_2 - k_{2H} m_5 - k_{3H} m_5 \tag{9e}$$
$$\dot{m}_6 = k_{1L} m_3 - k_{2L} m_6 - k_{3L} m_6 \tag{9f}$$
$$\dot{m}_7 = k_{2C} m_4 + k_{2H} m_5 + k_{2L} m_6 - k_4 m_7 \tag{9g}$$
$$\dot{m}_8 = (1 - Y_C) k_{3C} m_4 + (1 - Y_H) k_{3H} m_H + (1 - Y_L) k_{3L} m_6 - \Gamma \tag{9h}$$
$$\dot{m}_9 = Y_C k_{3C} m_4 + Y_H k_{3H} m_H + Y_L k_{3L} m_6 + \Gamma, \tag{9i}$$

where gamma is the rate at which char is formed in the pores in the biomass, per Xue et al. [25, 40],

$$\Gamma = \frac{\rho_g}{\rho_b} (\dot{m}_1 + \dot{m}_2 + \dot{m}_3 + \dot{m}_4 + \dot{m}_5 + \dot{m}_6) - \frac{\rho_g}{\rho_c} \dot{m}_9. \tag{10}$$

The first-order kinetic rates of Arrhenius form, $k_i = A_i \exp(E_i/(R_u T_b))$, are tabulated for each component in Table 3, and $R_u$ is the universal gas constant. The char formations ratios are $Y_C = 0.35$, $Y_H = 0.60$, and $Y_L = 0.75$, for cellulose, hemicellulose, and lignin, respectively [25, 29, 30, 34].

The time-rate-of-change of the enthalpy change for the conversion processes in Fig. 5 is $\Delta \dot{H}_P$ in Eq. 6. This value is calcu-

**TABLE 3**. KINETICS DATA

| Rate Constant | A (1/s) | E (MJ/kmol) | Reference |
|---|---|---|---|
| $k_{1C}$ | 2.80e19 | 242.4 | [25, 30] |
| $k_{2C}$ | 3.28e14 | 196.5 | [25, 30] |
| $k_{3C}$ | 1.30e10 | 150.5 | [25, 30] |
| $k_{1H}$ | 2.10e16 | 186.7 | [25, 29] |
| $k_{2H}$ | 8.75e15 | 202.4 | [25, 29] |
| $k_{3H}$ | 2.60e11 | 145.7 | [25, 29] |
| $k_{1L}$ | 9.60e8 | 107.6 | [25, 29] |
| $k_{2L}$ | 1.50e9 | 143.8 | [25, 29] |
| $k_{3L}$ | 7.70e6 | 111.4 | [25, 29] |
| $k_4$ | 4.25e6 | 108.0 | [25, 34] |

lated as

$$\Delta\dot{H}_P = \Delta\dot{H}_{\Delta htf} + \Delta\dot{H}_{\Delta gf} + \Delta\dot{H}_{\Delta cf} \tag{11a}$$

$$\Delta\dot{H}_{\Delta htf} = \Delta h_{tf}(k_{2C}m_4 + k_{2H}m_5 + k_{2L}m_6) \tag{11b}$$

$$\Delta\dot{H}_{\Delta hgf} = \Delta h_{gf}\dot{m}_8 \tag{11c}$$

$$\Delta\dot{H}_{\Delta hcf} = \Delta h_{cf}\dot{m}_9 \tag{11d}$$

where $\Delta h_{tf} = -255$ kJ/kg [37], $\Delta h_{gf} = 20$ kJ/kg [37], and $\Delta h_{cf} = 42$ kJ/kg [35] are the heats of reaction for tar, gas, and tar formation respectively. A negative sign indicates an endothermic reaction.

The combined natural/forced heat transfer coefficients are found from correlations [41]. The convection to the walls [42] and to the biomass [43] are assumed to be steady by non-dimensional analysis. Mass transfer will reduce the heat transfer coefficient to the biomass, so the high mass-transfer rate film theory correction [44, 45] is used as

$$\frac{h^*}{h} = \frac{\phi_T}{\exp(\phi_T) - 1}. \tag{12}$$

Here, $h^*$ and $h$ are the corrected and uncorrected heat transfer coefficients, respectively, and $\phi_T$ is defined as

$$\phi_T = \frac{\dot{m}_\phi c_{tv}}{A_s h}. \tag{13}$$

Here, $c_{tv}$ is the specific heat of the tar vapor, and $A_s$ is the surface area of the biomass particle. The mass loss from the biomass particle that is considered to reduce the heat transfer coefficient is $\dot{m}_\phi$ and may be written as

$$\begin{aligned}\dot{m}_\phi = k_{2C}m_4 + k_{2H}m_5 + k_{2L}m_6 + (1-Y_C)k_{3C}m_4 + \\ (1-Y_H)k_{3H}m_H + (1-Y_L)k_{3L}m_6\end{aligned} \tag{14}$$

Thermophysical properties for the fluidizing gas are calculated using Cantera [46] with the appropriate thermodynamic data [47] fitted to polynomials of temperature. The cylinder wall emissivity ($\varepsilon_w = 0.05$) is taken to be that of polished steel [48]. The biomass true density is assumed to be that of cellulose: $\rho_b = 1580$ kg/m$^3$ [49]. The specific heat of the biomass ($c_b$) is assumed to be that of cellulose

$$c_b = c_{gluc}(A + T_b B) \tag{15}$$

where $A = 0.9830$ J/mol-K and $B = 3.963$e-4 J/mol-K$^2$. The vibrational contribution to the heat capacity of glucose can be written as

$$c_{gluc} = \sum_i R_u \left(\frac{h\nu_i}{kT_b}\right)^2 \exp\left(\frac{h\nu_i}{kT_b}\right)\left(\left(\frac{h\nu_i}{kT_b}\right) - 1\right)^{-2} \tag{16}$$

where $R$ is the universal gas constant, $h$ is Planck's constant, $k$ is Boltzmann's constant, and $\nu_i$ is a frequency of the $i$th normal vibration [50].

Eqs. 5, 6, and 9 are implicit ordinary differential equations that are integrated in time to calculate the evolution of pressure, biomass temperature, fluidizing gas temperature, and conversion fractions for the compression and expansion strokes of the RBCR. The initial conditions are:

The biomass begins as virgin material (Fig. 5).
The initial biomass and fluidizing gas temperatures are $T_b = T_g = 22^\circ$C.
The mass of the biomass $m_b$ and the biomass radius $r_b$ are specified for one cycle.

MATLAB [51] is used to perform the integration for the implicit equations for prescribed cycle period which is determined by the engine speed; the results for the integrations presented herein are not sensitive to the ODE solver tolerance, bringing confidence in the calculation result.

## 6 CONVERSION OF BAGASSE IN A RBCR

In this section, we apply the model described in Sec. 5 to the decomposition of bagasse in a RBCR. The core of the reactor is assumed to be an 8-cylinder, 4-stroke, 7.3 L Diesel motor with a compression ratio of 21.5, modeled after the ubiquitous Ford 7.3 L Powerstroke Diesel Engine. A mixture of argon and spherical biomass particles 50 μm in diameter is injected into the intake of the engine. The composition of the biomass is split between cellulose, hemicellulose, and lignin to simulate bagasse decomposition (Table 1). The thermophysical properties of the biomass are assumed to be those of cellulose, per the discussion in Sec. 5.

Parameters and results for the decomposition of Bagasse are given in Table 4. Tabulated are: number of cylinders, bore, stroke, engine speed, mass flow of fluidizing gas $\dot{m}_{FG}$, volume-fraction of biomass $V_F$, the input energy per unit mass of biomass required to thermochemically convert the biomass $e_{in}$, and the feed rate of biomass $\dot{m}_b$.

**TABLE 4**. COMPARISON OF CALCULATED RBCR RESULTS WITH EXPERIMENTAL LAB-SCALE FLUIDIZED BED REACTOR RESULTS

| Parameter | RBCR | Lab FBR [21] |
|---|---|---|
| Cylinders | 8 | - |
| Bore | 104 mm | - |
| Stroke | 106 mm | - |
| RPM | 200 | - |
| $\dot{m}_{FG/CG}$ | 75 kg/hr (Ar) | 4.8 kg/hr ($N_2$) |
| $V_F$ | 74 ppm | 0.46 (wt/wt) |
| $\dot{m}_b$ | 5.3 kg/hr | 2.2 kg/hr |
| Feedstock | Bagasse | Switchgrass |
| $e_{in}$ | 2.1 MJ/kg | 3.5 MJ/kg |
| $\eta$ | 6.8 | 3.5 |
| Input particle diameter | 50 µm | <500 µm |

A figure of merit, termed 'return on energy investment,' is the ratio of power available from bio-oil out to the power required to operate the reactor, $\eta$, is written as

$$\eta = \frac{\dot{m}_b Q_{hv} Y_{tv/bo}}{\dot{Q}_{in}}, \tag{17}$$

where $Q_{hv} \approx 20$ MJ/kg is the heating value of bio-oil [52], $Y_{tv/bo}$ is the mass fraction of tar vapor or bio-oil for the calculations and the experimental results, respectively. The power supplied to the reactor is

$$\dot{Q}_{in} = \int_{\text{cycle}} pdV/t_{cycle} + \dot{m}_b e_{\text{comminute}}, \tag{18}$$

where the pressure-volume work per-unit cycle and power required to comminute the biomass to 50 µm are included. We conservatively estimate $e_{\text{comminute}} \approx 1$ MJ/kg by extrapolating from the values given in Mani et al. [53].

Experimental results from a lab-scale fluidized bed reactor (Lab FBR) are taken from the literature [21] for the purpose of comparison because they have nearly the same size/footprint and, thus, by crude assumption, similar capital costs.

A time-history of reactor pressure $P$, fluidizing gas temperature $T_g$, and biomass temperature $T_b$ for the reactor is presented as Fig. 6 for the compression and expansion strokes of the RBCR cycle. The maximum temperature of the biomass is over 500°C and the heating rate exceeds 5000°C/s during the compression stroke; these temperatures and heating rates are consistent with those found in the literature for fast pyrolysis [16]. The bio-products are rapidly cooled at over -5000°C/s during the expansion stroke; the rapid bio-product cooling rates will quench the undesirable secondary pyrolysis reactions. That is undesirable conversion from tar vapor to gas/char can be quenched (see Fig.5). For context, Boateng et al. [21] reports -60°C/s cooling in a bench-scale fluidized bed reactor with condensers packed with dry ice.

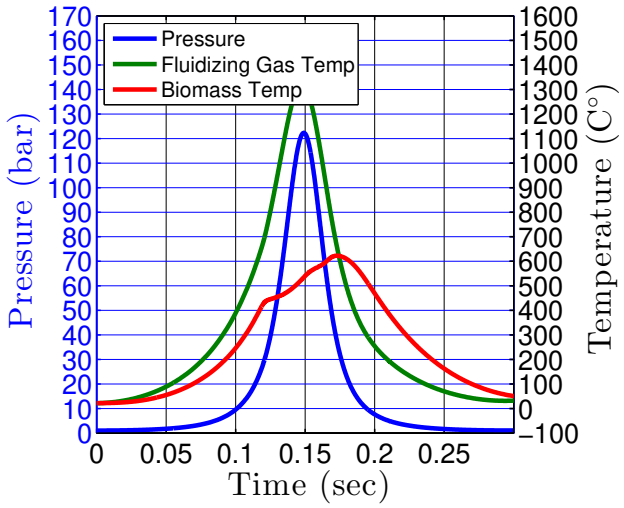


**FIGURE 6**. Compression (0-0.15 s) and expansion (0.15-0.30 s) strokes for the pilot-scale experiment. Calculation of reactor pressure $P$ (blue), fluidizing gas temperature$T_g$ (green), and biomass temperature $T_b$ (red).

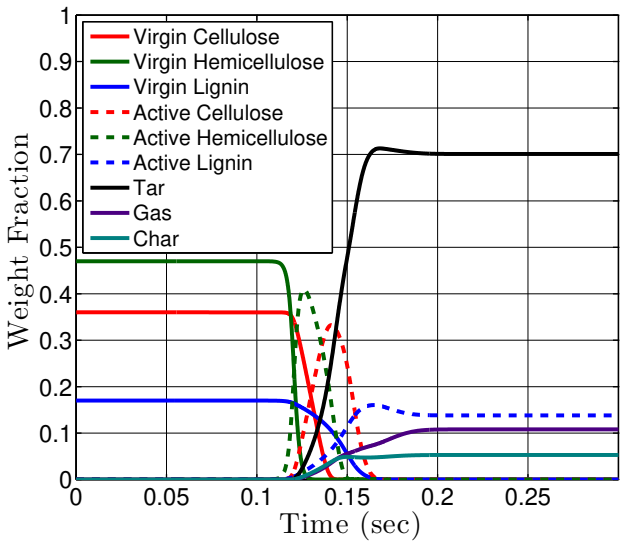


**FIGURE 7**. Compression(0-0.15 s) and expansion (0.15-0.30 s) strokes for the pilot-scale experiment. Calculated weight fractions vs. time per the model formulated in Sec. 5.

In Fig. 7, the biomass weight fraction evolution is presented per the model formulated in Sec. 5. The virgin/active cellulose and hemicellulose is degraded primarily between 0.10-0.20 s. The virgin lignin is degragded completely; however, there is still active lignin in the output of the reactor at this condition. This is unconverted biomass. At the end of an expansion stroke, ≈70% of the biomass is converted to pyrolysis vapor. Little undesirable secondary gas and char are produced because the rapid expansion stroke quenches all reactions within the cylinder.

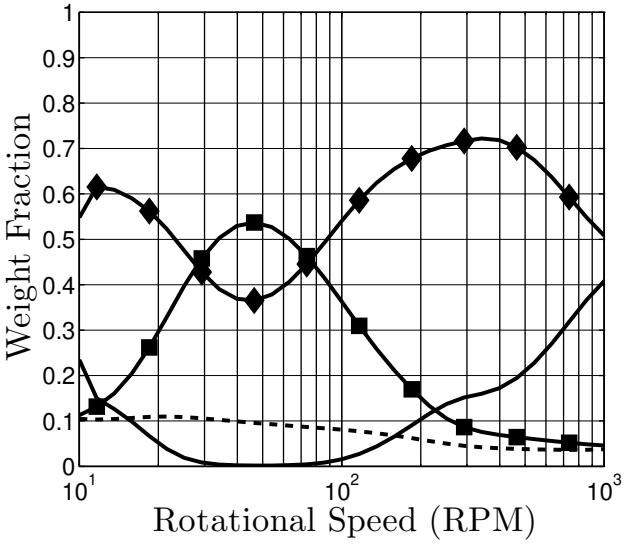


**FIGURE 8**. Weight fraction as a function of engine speed. Conversion fractions of tar vapor (♦ markers), gas (■ markers), char (no markers, dashed), and non-converted biomass (remaining virgin and active cellulose, hemicellulose, and lignin - no markers).

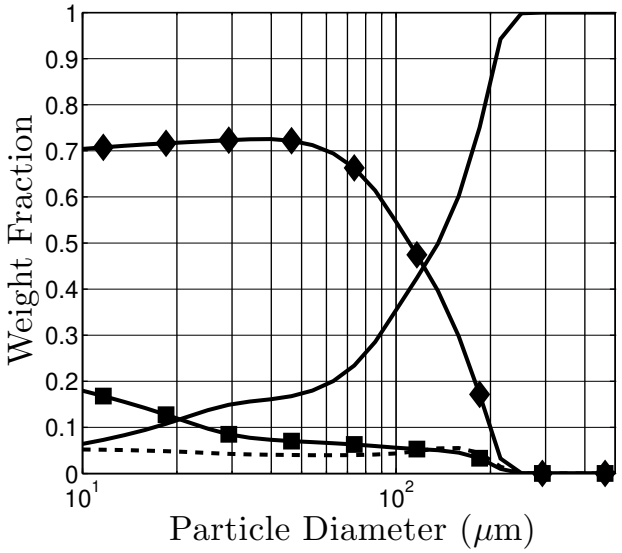


**FIGURE 9**. Conversion fraction as a function of particle diameter. Conversion fractions of tar vapor (♦ markers), gas (■ markers), char (no markers, dashed), and non-converted biomass (remaining virgin and active cellulose, hemicellulose, and lignin - no markers).

The disparity between the fluidizing gas temperature (green) and the biomass temperature (red) in Fig. 6 occurs between 0.10-0.20 s; the increase in biomass temperature appears to be stunted. It is during this time that the biomass is undergoing conversion (Fig. 7). Per the formulation in Sec. 5, the conversion process impedes heating because conversion to tar vapor is endothermic (per Eqs. 6 and 11b) and the heat transfer coefficient is reduced by film cooling (per Eqs. 12 and 13).

## 7 SENSITIVITY STUDY

In this section, a sensitivity study will be performed by fixing all but one parameter, namely engine speed, biomass particle diameter, biomass feed-rate, and biomass composition. The parameters and initial conditions are the same as in Section 6 and Table 4. The purpose of this exercise is to investigate how sensitive the RBCR concept is to variations in input conditions, and to aid in defining an intelligent operating parameter space.

In Fig. 8, the rotational speed is varied as all other parameters are fixed. The figure aids in defining the operating speed for the RBCR. Nearly complete conversion is calculated to occur for rotational speeds of 20-100 RPM, otherwise there is non-converted biomass within the cylinder after one cycle. The lower limit, 20 RPM, is a result of the higher fraction of input energy lost to heat transfer to the cylinder walls; that is, the compression stroke is highly non-adiabatic, and thus less energy is available for conversion. For engine speeds higher than 100 RPM, complete conversion cannot occur because of kinetic and heat transfer limitations. If the goal is to maximize the conversion of biomass to bio-oil, an engine speed of 200-500 RPM is appropriate to increase the yield of tar vapor, and maximize the throughput of the RBCR.

In Fig. 9, the biomass particle diameter is varied while all other parameters are held fixed. Calculations indicate that conversion decreases with increasing biomass diameter. The capability for the RBCR to convert biomass is reduced at a particle diameter of greater than 150 μm. The surface area available for heat transfer scales inversely with particle diameter. This inverse scaling overcomes the scaling of heat transfer coefficient with diameter. So, heat transfer to the biomass particle is calculated to be more efficient at smaller diameters, and this is the reason for the trends that appear in Fig. 9.

In Fig. 10, the biomass feed-rate is varied as the other parameters are held fixed. Calculations predict that complete conversion occurs for biomass feed-rates of less than 2 kg/hr. Decreasing the feed-rate far below 1 kg/hr is predicted to result in large fractions of bio-gas at the expense of tar vapor production. If the goal of the RBCR is to maximize bio-oil yield, the operational limit for biomass feed-rate would be 3-10 kh/hr to maximize the tar vapor yield. For this scale of RBCR, there is significant unconverted biomass at mass feed-rates of higher than 10 kg/hr.

In Fig. 11, the biomass composition fraction is varied. The initial composition is superimposed per Eq 8. Pure cellulose, bagasse, oak, and olive husk are considered. The feedstocks are chosen because of the increasing lignin content (see Table 1). Lignin is generally understood to make bio-oil production more difficult [1, 16]. It is calculated that cellulose is completely converted. The other feedstocks are not completely converted and the tar vapor weight fraction is reduced.

## 8 CONCLUSION

In this paper, a model is formulated for the decomposition of multi-component biomass in a reciprocating biomass conversion reactor (RBCR). A description of the decomposition of bagasse is presented for the compression and expansion strokes of the RBCR. Additionally, a sensitivity study was presented by fixing

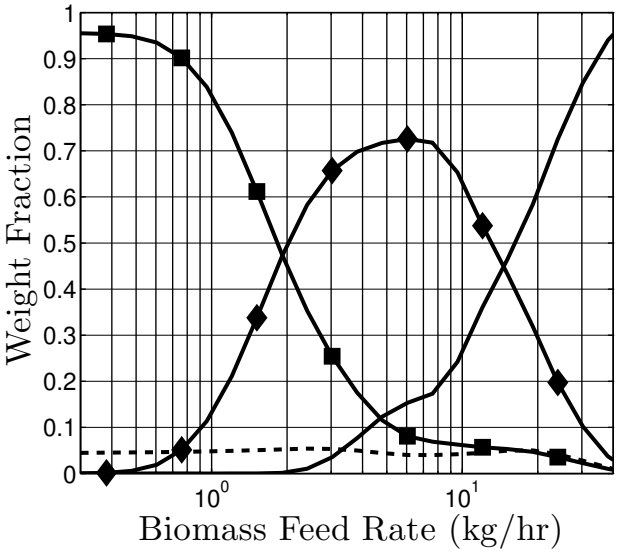


**FIGURE 10**. Conversion fraction as a function of biomass feed-rate. Conversion fractions of tar vapor (♦ markers), gas (■ markers), char (no markers, dashed), and non-converted biomass (remaining virgin and active cellulose, hemicellulose, and lignin - no markers).

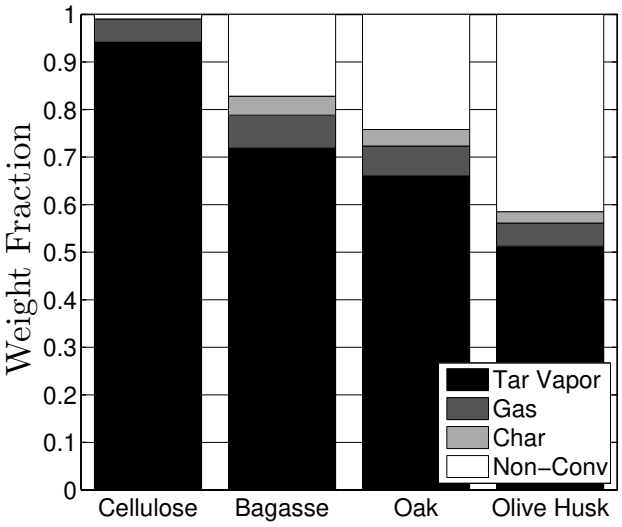


**FIGURE 11**. Conversion fractions of tar vapor, gas, char, and non-converted biomass. Mechanism shown in Fig. 5, and biomass compositions given in table 1.

all but one parameter, namely: engine speed, biomass particle diameter, biomass feed-rate, and biomass composition.

The calculations of baggase decomposition in the RBCR compare favorably to the experimental data for a lab scale fluidized bed reaction. This FBR was chosen because they have nearly the same size/footprint and, thus, by crude assumption, similar capital costs. Calculations indicate that the efficiency and 'return on energy investment' is increased by greater than ≈50%. The throughput also compares favorably to the FBR, as the RBCR is able to process significantly more biomass. Such efficiency and throughput increases would result in a decrease in the operational costs of biomass conversion. The RBCR permits control over the residence time within the reactor so that

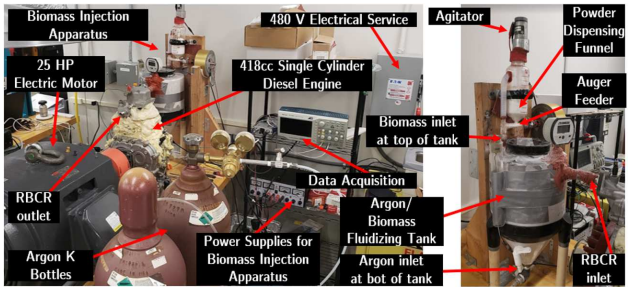


**FIGURE 12**. RBCR setup at Stevens Institute of Technology. Right: Close-up of the feeding/fluidization system.

unwanted reactions will not take place; this quenching occurs during the rapid expansion stroke in the RBCR. This process is in direct contrast to the FBR where the pyrolysis products must be processed by condensers to quench the unwanted secondary reactions; this process requires a longer time to undergo and there is an additional heat exchange.

The sensitivity study of the RBCR to input parameters indicates that the reactor is flexible in what it is able to accomplish. Preferential bio-gas or bio-oil production may be accomplished by adjusting the biomass feed-rate and engine speed. Engine speed and biomass feed-rate are relatively easily controlled relative to the calculated sensitivities.

The most significant limitation of this reactor is the sensitivity to particle size. Calculations predict that there will be significant fractions of unconverted biomass for particle sizes of greater than 150 μm. This size restriction poses an operational constraint as well as an additional overall energy input requirement to the conversion setup; although, even with this additional energy required for biomass pulverization, the RBCR compares favorably to the FBR.

Bagasse, oak, and olive husk were considered as candidates for RBCR feed-stock. It appears that bagasse is the strongest candidate because of its lower lignin content. The lower lignin content is possibly more important in the RBCR because of the shorter residence time than typically encountered in FBRs. Pure cellulose could be used as the feed-stock for RBCR development because it is easier to completely convert.

Currently at Stevens Institute of Technology, progress being made in the construction of the apparatus test bed, see Fig. 12. This RBCR is an inexpensive single-cylinder diesel engine that is used to compare to the model for performance predictions. Despite having similar cycles, the diesel engine is designed to operate under completely different conditions and therefore needs certain modifications to replicate the performance predicted by the model. We have identified the modifications required and verified their feasibility via experiments, and we are currently inching towards incorporating them in the RBCR with moderate success so far. Furthermore, conversion experiments have been performed with cellulose, and while the oil yield at the moment is expectedly lower than predicted by the model, preliminary tests/observations indicate that the oil produced could be of higher quality than common pyrolysis oil - probably due to rapid quenching of secondary pyrolysis. In addition, the various issues that could arise during prolonged operation of the RBCR and probable solutions have also been

considered. However, the in-depth analysis of these issues and the implementation of the solutions will have to wait until the RBCR is ready for such operation. A close-up of the feeding/fluidization system also appears as Fig. 12.

## ACKNOWLEDGMENT

Stevens Institute of Technology supported this work. The authors are also grateful for the support from the PSEG foundation to advance energy innovation at Stevens. We would also like to thank Prof. R. Besser for his helpful and insightful comments.

## REFERENCES

[1] Mohan, D., Pittman, C. U., and Steele, P. H., 2006. "Pyrolysis of Wood/Biomass for Bio-oil: A Critical Review". *Energy & Fuels,* ***20***(3), pp. 848–889.

[2] Wright, M., and Brown, R. C., 2007. "Establishing the optimal sizes of different kinds of biorefineries". *Biofuels, Bioproducts and Biorefining,* ***1***(3), pp. 191–200.

[3] Wright, M., Brown, R. C., and Boateng, A. A., 2008. "Distributed processing of biomass to bio-oil for subsequent production of fischer-tropsch liquids". *Biofuels, Bioproducts and Biorefining,* ***2***(3), pp. 229–238.

[4] Lehmann, J., Gaunt, J., and Rondon, M., 2006. "Biochar Sequestration in Terrestrial Ecosystems A Review". *Mitigation and Adaptation Strategies for Global Change,* ***11***(2), pp. 395–419.

[5] Lehmann, J., 2007. "A handful of carbon". *Nature,* ***447***(7141), pp. 143–144.

[6] Laird, D. A., 2008. "The charcoal vision: a win–win–win scenario for simultaneously producing bioenergy, permanently sequestering carbon, while improving soil and water quality". *Agronomy Journal,* ***100***(1), pp. 178–181.

[7] Laird, D. A., Brown, R. C., Amonette, J. E., and Lehmann, J., 2009. "Review of the pyrolysis platform for coproducing bio-oil and biochar". *Biofuels, Bioproducts and Biorefining,* ***3***(5), pp. 547–562.

[8] Lee, J. W., Hawkins, B., Day, D. M., and Reicosky, D. C., 2010. "Sustainability: the capacity of smokeless biomass pyrolysis for energy production, global carbon capture and sequestration". *Energy & Environmental Science,* ***3***(11), pp. 1695–1705.

[9] Woolf, D., Amonette, J. E., Street-Perrott, F. A., Lehmann, J., and Joseph, S., 2010. "Sustainable biochar to mitigate global climate change". *Nature communications,* ***1***, p. 56.

[10] Brown, R. C., 2009. "Biochar Production Technology". In *Lehmann, J. and Joseph, S.*, Biochar for Environmental Management: Science and Technology, ed. Earthscan.

[11] Krieger-Brockett, B., 1994. "Microwave pyrolysis of biomass". *Research on Chemical Intermediates,* ***20***(1), pp. 39–49.

[12] Meier, D., and Faix, O., 1999. "State of the art of applied fast pyrolysis of lignocellulosic materials - a review". *Bioresource Technology,* ***68***(1), pp. 71–77.

[13] Czernik, S., and Bridgwater, A. V., 2004. "Overview of applications of biomass fast pyrolysis oil". *Energy & Fuels,* ***18***(2), pp. 590–598.

[14] Bridgwater, A. V., Meierb, D., and Radlein, D., 1999. "An overview of fast pyrolysis of biomass". *Organic Geochemistryy,* ***30***, pp. 1479–1493.

[15] Bridgwater, A. V., and Peacocke, G. V. C., 2000. "Fast pyrolysis processes for biomass". *Renewable and Sustainable Energy Reviews,* ***4***(1), pp. 1–73.

[16] Bridgwater, A. V., 2012. "Review of fast pyrolysis of biomass and product upgrading". *Biomass and Bioenergy,* ***38***, pp. 68–94.

[17] Zhang, Q., Chang, J., Wang, T., and Xu, Y., 2007. "Review of biomass pyrolysis oil properties and upgrading research". *Energy Conversion and Management,* ***48***(1), pp. 87–92.

[18] Babu, B. V., 2008. "Biomass pyrolysis: a state-of-the-art review". *Biofuels, Bioproducts and Biorefining,* ***2***(5), pp. 393–414.

[19] Goyal, H. B., Seal, D., and Saxena, R. C., 2008. "Bio-fuels from thermochemical conversion of renewable resources: a review". *Renewable and Sustainable Energy Reviews,* ***12***(2), pp. 504–517.

[20] Jun, D., L., P., Zuo-hua, L., gui S., D., and yuan T., C., 2010. "Fast pyrolysis of biomass for bio-oil with ionic liquid and microwave irradiation". *Journal of Fuel Chemistry and Technology,* ***38***(5), pp. 554–559.

[21] Boateng, A. A., Daugaard, D. E., Goldberg, N. M., and Hicks, K. B., 2007. "Bench-Scale Fluidized-Bed Pyrolysis of Switchgrass for Bio-Oil Production". *Industrial & Engineering Chemistry Research,* ***46***(7), pp. 1891–1897.

[22] Parziale, N. J., 2014. "Thermo-chemical biomass conversion by piston compression of surrounding gas". In Proceedings of the 247th American Chemical Society National Meeting, ACS-ENFL-69.

[23] Parziale, N. J., 2014. "Calculation of Input Sensitivities for a Reciprocating Biomass Conversion Reactor (RBCR)". In Proceedings of the 3rd International Energy and Sustainability Conference, IEEE.

[24] van Basshuysen, R., and Schäfer, F., 2004. *Internal Combustion Engine Handbook - Basics, Components, Systems, and Perspectives*. Society of Automotive Engineers, Inc.

[25] Xue, Q., Heindel, T. J., and Fox, R. O., 2011. "A CFD model for biomass fast pyrolysis in fluidized-bed reactors". *Chemical Engineering Science,* ***66***(11), pp. 2440–2452.

[26] Antal Jr., M. J., and Várhegyi, G., 1995. "Cellulose Pyrolysis Kinetics: The Current State of Knowledge". *Industrial & Engineering Chemistry Research,* ***34***(3), pp. 703–717.

[27] Várhegyi, G., Antal Jr., M. J., Jakab, E., and Szabó, P., 1997. "Kinetic modeling of biomass pyrolysis". *Journal of Analytical and Applied Pyrolysis,* ***42***(1), pp. 73–87.

[28] Di Blasi, C., 2008. "Modeling chemical and physical processes of wood and biomass pyrolysis". *Progress in Energy and Combustion Science,* ***34***(1), pp. 47–90.

[29] Miller, R. S., and Bellan, J., 1997. "A generalized biomass pyrolysis model based on superimposed cellulose, hemicellulose and liqnin kinetics". *Combustion Science and Technology,* ***126***(1-6), pp. 97–137.

[30] Bradbury, A. G. W., Sakai, Y., and Shafizadeh, F., 1979.

"A kinetic model for pyrolysis of cellulose". *Journal of Applied Polymer Science,* ***23***(11), pp. 3271–3280.

[31] Shafizadeh, F., and Bradbury, A. G. W., 1979. "Thermal degradation of cellulose in air and nitrogen at low temperatures". *Journal of Applied Polymer Science,* ***23***(5), pp. 1431–1442.

[32] Shafizadeh, F., 1982. "Introduction to pyrolysis of biomass". *Journal of Analytical and Applied Pyrolysis,* ***3***(4), pp. 283–305.

[33] Ward, S. M., and Braslaw, J., 1985. "Experimental weight loss kinetics of wood pyrolysis under vacuum". *Combustion and flame,* ***61***(3), pp. 261–269.

[34] Liden, A. G., Berruti, F., and Scott, D. S., 1988. "A kinetic model for the production of liquids from the flash pyrolysis of biomass". *Chemical Engineering Communications,* ***65***(1), pp. 207–221.

[35] Curtis, L. J., and Miller, D. J., 1988. "Transport Model with Radiative Heat Transfer for Rapid Cellulose Pyrolysis". *Industrial & Engineering Chemistry Research,* ***27***(10), pp. 1775–1783.

[36] Koufopanos, C. A., Lucchesi, A., and Maschio, G., 1989. "Kinetic Modelling of the Pyrolysis of Biomass and Biomass Components". *The Canadian Journal of Chemical Engineering,* ***67***(1), pp. 75–84.

[37] Koufopanos, C. A., Papayannakos, N., Maschio, G., and Lucchesi, A., 1991. "Modelling of the Pyrolysis of Biomass Particles. Studies on Kinetics, Thermal and Heat Transfer Effects". *The Canadian Journal of Chemical Engineering,* ***69***(4), pp. 907–915.

[38] Di Blasi, C., 1994. "Numerical simulation of cellulose pyrolysis". *Biomass and Bioenergy,* ***7***(1-6), pp. 87–98.

[39] Milosavljevic, I., and Suuberg, E. M., 1995. "Cellulose Thermal Decomposition Kinetics: Global Mass Loss Kinetics". *Industrial & Engineering Chemistry Research,* ***34***(4), pp. 1081–1091.

[40] Xue, Q., Dalluge, D., Heindel, T. J., Fox, R. O., and Brown, R. C., 2012. "Experimental validation and CFD modeling study of biomass fast pyrolysis in fluidized-bed reactors". *Fuel,* ***97***, pp. 757–769.

[41] Incropera, F. P., DeWitt, D. P., Bergman, T. L., and Lavine, A. S., 2007. *Fundamentals of Heat and Mass Transfer*, sixth ed. John Wiley & Sons Incorporated.

[42] Patterson, J., and Imberger, J., 1980. "Unsteady natural convection in a rectangular cavity". *Journal of Fluid Mechanics,* ***100***(1), pp. 65–86.

[43] Dudek, D. R., Fletcher, T. H., Longwell, J. P., and Sarofim, A. F., 1988. "Natural convection induced drag forces on spheres at low grashof numbers: comparison of theory with experiment". *International Journal of Heat and Mass Transfer,* ***31***(4), pp. 863–873.

[44] Bird, R. B., Stewart, W. E., and Lightfoot, E. N., 1960. *Transport Phenomena*, 1st ed. John Wiley & Sons.

[45] Lienhard, J. H., 2012. *A Heat Transfer Textbook*, 4th ed. Phlogiston Press.

[46] Goodwin, D. G., 2003. "An Open-Source, Extensible Software Suite for CVD Process Simulation". In Proceedings of CVD XVI and EuroCVD Fourteen, M Allendorf, F Maury, and F Teyssandier (Eds.), pp. 155–162.

[47] McBride, B. J., Zehe, M. J., and Gordon, S., 2002. NASA Glenn Coefficients for Calculating Thermodynamic Properties of Individual Species. NASA TP-2002-211556.

[48] Çengel, Y. A., and Ghajar, A. J., 2011. *Heat and Mass Transfer: Fundamentals & Applications*, fourth ed. McGraw-Hill.

[49] Sun, C. C., 2005. "True density of microcrystalline cellulose". *Journal of Pharmaceutical Sciences,* ***94***(10), pp. 2132–2134.

[50] Blokhin, A. V., Voitkevich, O. V., Kabo, G. J., Paulechka, Y. U., Shishonok, M. V., Kabo, A. G., and Simirsky, V. V., 2011. "Thermodynamic Properties of Plant Biomass Components. Heat Capacity, Combustion Energy, and Gasification Equilibria of Cellulose". *Journal of Chemical & Engineering Data,* ***56***(9), pp. 3523–3531.

[51] Shampine, L. F., and Reichelt, M. W., 1997. "The Matlab ODE Suite". *SIAM Journal on Scientific Computing,* ***18***(1), pp. 1–22.

[52] Mullen, C. A., Boateng, A. A., Goldberg, N. M., Lima, I. M., Laird, D. A., and Hicks, K. B., 2010. "Bio-oil and bio-char production from corn cobs and stover by fast pyrolysis". *Biomass and Bioenergy,* ***34***(1), pp. 67–74.

[53] Mani, S., Tabil, L. G., and Sokhansanj, S., 2004. "Grinding performance and physical properties of wheat and barley straws, corn stover and switchgrass". *Biomass and Bioenergy,* ***27***(4), pp. 339–352.